

# Elliptic flow of thermal photons at midrapidity in Au+Au collisions at $\sqrt{s_{NN}} = 200$ GeV

Fu-Ming Liu<sup>a</sup>, Tetsufumi Hirano<sup>b</sup>, Klaus Werner<sup>c</sup>, Yan Zhu<sup>a</sup>

<sup>a</sup>*Institute of Particle Physics, Central China Normal University, 430079, Wuhan, China*

<sup>b</sup>*Department of Physics, The University of Tokyo, 113-0033, Japan*

<sup>c</sup>*Laboratoire SUBATECH, University of Nantes - IN2P3/CNRS - Ecole des Mines, Nantes, France*

## Abstract

The elliptic flow  $v_2$  of thermal photons at midrapidity in Au+Au collisions at  $\sqrt{s_{NN}} = 200$  GeV is predicted, based on three-dimensional ideal hydrodynamics. Because of the interplay between the asymmetry and the strength of the transverse flow, the thermal photon  $v_2$  reaches a maximum at  $p_T \sim 2\text{GeV}/c$  and the  $p_T$ -integrated  $v_2$  reaches a maximum at about 50% centrality. The  $p_T$ -integrated  $v_2$  is very sensitive to the lower limit of the integral but not sensitive to the upper limit due to the rapid decrease in the spectrum of the transverse momentum.

## 1. Introduction

The deconfined and novel nuclear matter, the quark gluon plasma (QGP), has been expected to appear in relativistic heavy ion collisions. The observation of large elliptic flow of different hadronic species at the Relativistic Heavy Ion Collider (RHIC) at Brookhaven National Lab, New York, is of special importance to confirm the formation of QGP. Unlike those bulk hadrons, photons are produced during the whole history of the evolution of the hot and dense matter. Moreover, the mean free path of photons is much larger than the transverse size of the bulk matter. So the produced photons pass through the surrounding matter without any interaction. As a result, thermal photons provide undistorted information on flow asymmetries not only from its surface but also from the inner of the hot, dense matter.

Therefore the question such as what is the relation between the measurable elliptic flow  $v_2$  of thermal photons and the evolution process of the expanding hot dense matter is of interest. This relation will serve as a direct bridge between the observables and the properties of the quark gluon plasma. A pioneering work has been done based on 2D ideal hydrodynamics, which has shown the transverse momentum and centrality dependence of the elliptic flow of thermal photons at midrapidity[1]. In this paper, the elliptic flow of thermal photons is calculated based on 3D ideal hydrodynamics. The paper is organized as following. In Sec. 2 we will briefly review the space-time evolution of the hot and dense matter using 3D ideal hydrodynamics and the basic formula for the production of thermal photons. In Sec. 3, we will show our results on the transverse momentum and centrality dependences of thermal photons  $v_2$  in Au+Au collisions at  $\sqrt{s_{NN}} = 200$  GeV. Section 4 is devoted to discussion and summary of our results.

## 2. Bulk evolution, thermal photons, and elliptic flow

In our calculation, a full 3D ideal hydrodynamic calculation is employed to describe the space-time evolution of the hot and dense matter created in Au+Au collisions at RHIC. The impact parameters corresponding to different centralities in Au+Au collisions at RHIC, which are estimated with a Glauber model, are 3.2, 5.5, 7.2, 8.5, 9.7, 10.8, and 11.7 fm for 0-10%, 10-20%, ... and 60-70% centrality, respectively. The local thermal equilibrium is assumed to be reached at the initial time  $\tau_0 = 0.6 \text{ fm}/c$ . The critical temperature of a first order phase transition between the QGP phase and the hadron phase is fixed at  $T_c = 170 \text{ MeV}$ . The initial flow is taken to be Bjorken scaling solution. So the transverse flow is vanishing at  $\tau_0$  and dynamically generated by the pressure gradient. More details can be found in [2, 3].

Transverse momentum spectra of thermal photons can be written as

$$\frac{dN}{dy d^2 p_t} = \int d^4 x \Gamma(E^*, T) \quad (1)$$

with  $\Gamma(E^*, T)$  being the Lorentz invariant thermal photons emission rate,  $d^4 x = \tau d\tau dx dy d\eta$  being the volume-element, the integration is done from the initial time  $\tau_0$  to the freeze-out, and  $E^* = p^\mu u_\mu$  the photon energy in the local rest frame. More details can be found in [4].

The elliptic flow is quantified by the second harmonic coefficient  $v_2$

$$v_2(p_T, y) = \frac{\int d\phi \cos(2\phi) d^3 N / dy d^2 p_t}{\int d\phi d^3 N / dy d^2 p_t}, \quad (2)$$

where  $\phi$  is the azimuthal angle of photon's momentum with respect to the reaction plane.

The  $p_t$  dependence of the triple differential spectra is strongly affected by the flow  $u$  through the argument  $E^* = p^\mu u_\mu$  in the photon emission rate. The azimuthal asymmetry of the transverse components of the flow obviously results in an anisotropic momentum distribution, which gives a finite  $v_2$ . Therefore both strength and the anisotropy of transverse flow velocity are important to generate the elliptic flow of thermal photons. The two key features of QGP, mean radial flow  $\langle v_r \rangle$  and the mean anisotropy of flow  $\langle v_2^{\text{hydro}} \rangle$ , are defined as

$$\langle v_r \rangle = \left\langle \sqrt{v_x^2 + v_y^2} \right\rangle, \quad \langle v_2^{\text{hydro}} \rangle = \left\langle \frac{v_x^2 - v_y^2}{v_x^2 + v_y^2} \right\rangle, \quad (3)$$

where  $\langle \dots \rangle$  stands for energy-density-weighted space-time average,  $v_x$  and  $v_y$  are the flow velocity components along  $x$ -axis and  $y$ -axis, respectively. From Table 1, we see that the mean radial flow increases with centrality from 0-10% ( $b = 3.2 \text{ fm}$ ) to 20-30% ( $b = 7.2 \text{ fm}$ ), then decreases from 20-30% ( $b = 7.2 \text{ fm}$ ) to 60-70% ( $b = 11.7 \text{ fm}$ ). On the other hand, the mean flow anisotropy increases with centrality from 0-10% to 60-70% monotonically. The increase of the average radial flow between 0-10% and 20-30% can be understood due to the fact that the initial shape of matter becomes more asymmetric, leading to flow asymmetry, as discussed earlier. The decrease beyond 20-30% is due to the decreasing life times, which prevents large flows from developing.

## 3. Results

In Fig. 1, the  $v_2$  of thermal photons at midrapidity  $y = 0$  in  $0 < p_T < 6 \text{ GeV}/c$  is shown for various centralities from 0 to 70% in Au+Au collisions at  $\sqrt{s_{NN}} = 200 \text{ GeV}$ . The solid lines from

Table 1: The strength and the anisotropy of transverse flow at each centrality.

Centrality(%)	0-10	10-20	20-30	30-40	40-50	50-60	60-70
$b(\text{fm})$	3.2	5.5	7.2	8.5	9.7	10.8	11.7
$\langle v_r \rangle$	0.114	0.122	0.123	0.117	0.109	0.0959	0.0804
$\langle v_2^{\text{hydro}} \rangle$	0.0417	0.103	0.154	0.188	0.212	0.222	0.240

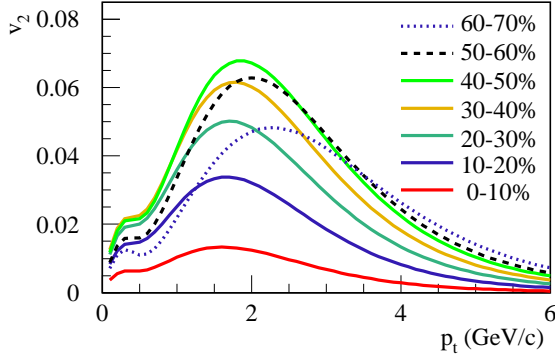


Figure 1: (Color online) Midrapidity  $v_2$  for thermal photons in Au+Au collisions at  $\sqrt{s_{NN}} = 200$  GeV is shown for various centralities from 0 to 70% in  $0 < p_T < 6$  GeV/c.

bottom to top refer to centralities 0-10%, 10-20%, 20-30%, 30-40%, and 40-50%, respectively. The dashed lines from top to bottom at  $p_T = 2$  GeV/c refer to the centralities 50-60% and 60-70%.

For each centrality, the thermal  $v_2$  increases then decreases with increasing  $p_t$  and a peak appears at  $p_t \sim 2$  GeV/c. This  $p_t$  dependence is consistent with the prediction based on 2+1D hydrodynamics[1] and explained as the weak transverse flow at the early stage.

The centrality dependence is shown clearly in Fig. 2, where the  $p_T$ -integrated  $v_2$  at  $y = 0$  is plotted as a function of impact parameter  $b$ . The  $p_T$ -integrated  $v_2$  reaches maximum at about 50% centrality, due to the interplay between the asymmetry and the strength of the transverse flow, as shown in Tab.I.

In Fig. 2, the dependence of  $p_T$ -integrated range is presented with various types of curves. The  $p_T$ -integrated  $v_2$  is not sensitive to the upper limit, as one can see that the curves from integrated range (0,3) and (0,6)GeV do not differ. But it is very sensitive to the lower limit, as shown in Fig. 2, where three lower limits of  $p_T$ -integral, 0, 0.5 and 1GeV/c, are used. The reason is that the  $p_T$  spectrum of thermal photons decreases so rapidly[4] that the  $v_2$  weight at low  $p_T$  spectrum plays an very important role.

#### 4. Conclusion

Based on a three-dimensional ideal hydrodynamics, we calculated the elliptic flow of thermal photons  $v_2$  from Au+Au collisions at  $\sqrt{s_{NN}} = 200$  GeV. Due to the interplay between the asymmetry and the strength of the transverse flow, thermal photon  $v_2$  reaches maximum at  $p_T \sim 2$ GeV/c and  $p_T$ -integrated  $v_2$  reaches maximum at about 50% centrality.

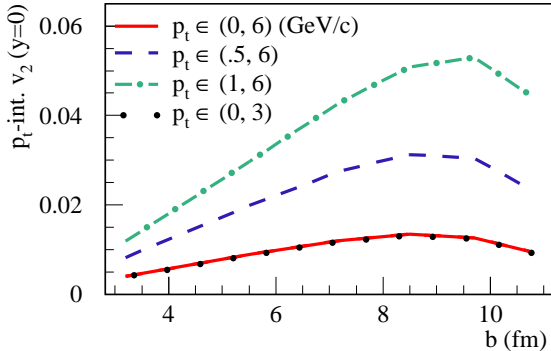


Figure 2: (Color online) The  $p_T$ -integrated  $v_2$  at  $y = 0$  is plotted as a function of impact parameter  $b$ . The dependence of  $p_T$ -integrated range is presented with various types of curves.

The insensitivity of the  $p_T$ -integrated  $v_2$  to upper  $p_T$ -integral limit is very useful. In fact if we include all sources of direct photons, the  $p_T$ -integrated  $v_2$  will not differ much, for two reasons:  
1) The yield of direct photons at higher  $p_T$  is small because the  $p_T$  spectrum of direct photons decreases rapidly though all sources of direct photons are counted[4].  
2) The  $v_2$  is also very small at higher  $p_T$  for obvious reason that the main contribution at high  $p_T$ , the leading order contribution from nucleon-nucleon collisions, has a vanishing  $v_2$ .  
So we can predict the  $p_T$ -integrated  $v_2$  are dominated by thermal photons.

The  $p_T$ -integrated  $v_2$  is very sensitive to the lower integral limit. Experimentally, the smallest measurable  $p_T$  is up to the detector. Above this value, experimentalists can still vary the lower integral limit of  $p_T$  to check how reliable the photon emission rate formula is. Theoretically this formula is very close to non-perturbative region and not reliable.

Though 3D hydrodynamics provides similar results as from 2D hydrodynamics at midrapidity, the rapidity dependence will be certainly different, which will be presented later.

### Acknowledgments

This work is supported by the Natural Science Foundation of China under the project No. 10505010 and MOE of China under project No. IRT0624. The work of T.H. was partly supported by Grant-in-Aid for Scientific Research No. 19740130 and by Sumitomo Foundation No. 080734. FML is particularly grateful to U. Heinz, R. Chatterjee and D. K. Srivastava, for the helpful discussion.

### References

- [1] R. Chatterjee, E. Frodermann, U. Heinz, and D.K. Srivastava, Phys. Rev. Lett. **96**, 202302 (2006).
- [2] T. Hirano, Phys. Rev. C **65**, 011901 (2002).
- [3] T. Hirano and K. Tsuda, Phys. Rev. C **66**, 054905 (2002).
- [4] F. M. Liu, T. Hirano, K. Werner and Y. Zhu, Phys. Rev. C **79**, 014905 (2009)